


Modelling the distribution of hard seabed using calibrated multibeam acoustic backscatter data in a tropical, macrotidal embayment: Darwin Harbour, Australia

P. Justy W. Siwabessy¹  · Maggie Tran¹ · Kim Picard¹ · Brendan P. Brooke¹ · Zhi Huang¹ · Neil Smit² · David K. Williams³ · William A. Nicholas¹ · Scott L. Nichol¹ · Ian Atkinson¹

Received: 15 November 2016 / Accepted: 3 May 2017 / Published online: 9 May 2017
© The Author(s) 2017. This article is an open access publication

Abstract Spatial information on the distribution of seabed substrate types in high use coastal areas is essential to support their effective management and environmental monitoring. For Darwin Harbour, a rapidly developing port in northern Australia, the distribution of hard substrate is poorly documented but known to influence the location and composition of important benthic biological communities (corals, sponges). In this study, we use angular backscatter response curves to model the distribution of hard seabed in the subtidal areas of Darwin Harbour. The angular backscatter response curve data were extracted from multibeam sonar data and analysed against backscatter intensity for sites observed from seabed video to be representative of “hard” seabed. Data from these sites were consolidated into an “average curve”, which became a reference curve that was in turn compared to all other angular backscatter response curves using the Kolmogorov–Smirnov goodness-of-fit. The output was used to generate interpolated spatial predictions of the probability of hard seabed (p -hard) and derived hard seabed parameters for the mapped area of

Darwin Harbour. The results agree well with the ground truth data with an overall classification accuracy of 75% and an area under curve measure of 0.79, and with modelled bed shear stress for the Harbour. Limitations of this technique are discussed with attention to discrepancies between the video and acoustic results, such as in areas where sediment forms a veneer over hard substrate.

Keywords Multibeam · Acoustics · Bathymetry · Backscatter · Angular backscatter response

Introduction

Managers are often faced with making a myriad of decisions about how best to sustainably manage marine and coastal assets. Many decisions are based on questions such as “where are ecologically significant areas located?”; “what are the potential impacts of proposed coastal developments and how can these be mitigated?”;

✉ P. Justy W. Siwabessy
Justy.Siwabessy@ga.gov.au

Maggie Tran
Maggie.Tran@ga.gov.au

Kim Picard
Kim.Picard@ga.gov.au

Brendan P. Brooke
Brendan.Brooke@ga.gov.au

Zhi Huang
Zhi.Huang@ga.gov.au

Neil Smit
Neil.Smit@nt.gov.au

David K. Williams
DK.Williams@aims.gov.au

William A. Nicholas
Tony.Nicholas@ga.gov.au

Scott L. Nichol
Scott.Nichol@ga.gov.au

Ian Atkinson
Ian.Atkinson@ga.gov.au

¹ Geoscience Australia, GPO Box 378, Canberra, ACT 2601, Australia

² Department of Environment and Natural Resources, Northern Territory Government, PO Box 496, Palmerston, NT 0831, Australia

³ Australian Institute of Marine Science, PO Box 41775, Casuarina, NT 0811, Australia

“what robust monitoring programs are needed to monitor changes over time and thus gauge the effectiveness of management decisions?” To address these types of questions requires a foundation of baseline environmental information, in particular water column characteristics and the character and distribution of seabed substrate types and associated biological communities.

The spatial distribution of seabed habitats and species, and composition of species assemblages at local and regional scales are shaped by physical and chemical environmental characteristics, such as temperature, salinity, water depth, light availability, current strength (bed shear stress), sediment texture and composition, and geomorphology (e.g. Gray 1974; Guisan and Zimmermann 2000; Kostylev et al. 2001; Brown and Collier 2008). Furthermore, the presence of species-rich areas and biodiversity hot spots is often associated with habitat heterogeneity, substrate characteristics and topographic complexity (e.g. Ke et al. 1994; Green et al. 1998; Peterson et al. 1998; Garza-Perez et al. 2004; Beaman et al. 2005; Post et al. 2006; Wedding et al. 2008; McArthur et al. 2010; Guevara-Fletcher et al. 2011; Nichol et al. 2012; Przeslawski et al. 2011, 2015). In particular, hard seabed areas, either as exposed rock or sediment veneer overlying rocky substrates, provide habitat for distinct benthic communities and are often more species diverse compared to adjacent unconsolidated or flat seabed (Banks et al. 2008; McArthur et al. 2010).

Hard substrate with its physical complexity, stability and associated interaction with bottom currents provides habitat and food for sessile biota and a range of other organisms (Greene et al. 2007; Kracker et al. 2008; Wedding et al. 2008). It also offers refuge from predators and settlement surfaces not available on flat seabed (Reise 1981; Tsuchiya and Nishihira 1986; Nakamura and Sano 2005; Callaway 2006), provides habitat structure for juvenile and adult animals (Kostylev et al. 2003) and influences foraging patterns (Erlandsson et al. 1999). To facilitate mapping of hard substrates, reproducible seabed classification methods are needed. Geophysical datasets such as multibeam sonar bathymetry and backscatter can be employed to identify and map these potentially biologically-important seabed types. Multibeam bathymetry data have been extensively used to provide spatially continuous variables that describe the morphology of the seabed, which have in turn been used as surrogates of biodiversity (Harris 2012; examples in; Harris and Baker 2012). Seabed parameters that can be derived from multibeam backscatter data are also widely utilised. For example, finer-grained (muddy) sediments generally produce low acoustic returns (backscatter), whereas coarser (sandy) sediments and rock outcrops are more likely to produce higher acoustic returns.

Multibeam sonar instruments acquire co-located seabed bathymetry and backscatter data over port and starboard orientated swath, varying between widths of 120° and 150° (Hughes-Clarke 1994). Theoretical models and experimental observations demonstrate that acoustic backscatter from the seabed is a complex function of many factors, such as incidence angle, acoustic frequency, roughness scales, grain-size distribution, presence of fauna and flora, biological reworking, and volume reverberation (Jackson et al. 1986, 1996; de Moustier and Alexandrou 1991; Lyons et al. 1994, APL 1994; Hughes-Clarke 1994; Talukdar et al. 1995; Novarini and Caruthers 1998; Williams et al. 2002; Siwabessy et al. 2006a, b; Fonseca and Mayer 2007; Parnum 2007; De Falco et al. 2010; Gavrilov and Parnum 2010; Hamilton and Parnum 2011; Hasan et al. 2012; Lurton and Lamarche 2015). Of these factors, the incidence angle is of primary importance, with backscatter strength near the nadir (i.e. at small incidence angles) generally higher than that recorded in the outer swath because of the differences between reflection (near nadir) and scattering (outer swath) (de Moustier and Alexandrou 1991; Ferrini and Flood 2006). These nadir reflections thus cause difficulty in characterising patterns in seabed substrate. The variation of backscatter values, over a continuous range of incidence angles, is referred to as an angular backscatter response. The angular backscatter response is considered an intrinsic property of the seabed which can be used as a primary means of seabed characterisation (Hughes-Clarke et al. 1997; Canepa and Pace 2000; Parnum et al. 2004, 2006; Fonseca and Mayer 2007; Gavrilov and Parnum 2010; Hamilton and Parnum 2011; Huang et al. 2013, 2014; Daniell et al. 2015). For instance, sand-covered and mud-covered seabed show a rapid decrease in the backscatter strength toward the outer swath angles, whereas dense seagrass beds produces backscatter strength almost independent of the incidence angle (Siwabessy et al. 2006b).

Angular backscatter response analysis utilises the full response curve to segment the seabed into regions with similar acoustic properties (de Moustier and Matsumoto 1993; Hughes-Clarke et al. 1997; Fonseca and Mayer 2007). Unlike pixel-based classification methods, angular response analysis is limited to two rectangular footprints on either side of the multibeam swath. Therefore, angular response analysis is most effective where it is valid to assume homogeneity of the seabed in the half-swath width (Hughes-Clarke et al. 1997). While the angular backscatter response offers greater angular resolution than backscatter mosaics can provide, it is lower in spatial resolution than backscatter mosaics.

Several shape parameters (e.g. slope, intercept and average within a certain domain interval of incidence angles) can be extracted from multibeam sonar angular backscatter response curves as inputs to the models that predict various

seabed geophysical properties and substratum types (Fonseca and Mayer 2007; Fonseca et al. 2009; Lamarche et al. 2010; Huang et al. 2013, 2014). This prediction approach has shown promise for seabed habitat mapping applications, although it is yet to be tested over a range of benthic marine environments and acoustically complex sediments such as coarse-grained carbonates (Brown et al. 2011).

Hamilton and Parnum (2011) argued that the direct clustering of angular backscatter response curves is able to form a standalone, independent map of seabed acoustic properties. The virtues of direct clustering lie in the use of actual angular backscatter response curves and its simple and rapid computation. However, the resultant acoustic classes need extra information to be assigned meaningful seabed types. Huang et al. (2013), instead, used a supervised approach to directly classify the seabed into various substrate types, based on angular backscatter response curves and ground truth samples. The classification results of their study indicate a moderate to high classification accuracy when this approach is used.

Here, we demonstrate a method for predicting the distribution of hard substrate in a shallow, turbid, macro-tidal embayment using multibeam acoustic data in combination with seabed samples and video images of the seabed. We adopt a supervised approach to the angular backscatter response curves of the half-swath width using the Kolmogorov–Smirnov goodness of fit test. This test has been used in a number of studies involving backscatter strength statistics and their distribution model for different seabed types on multiple incidence angle domains (Jakeman and Tough 1988; Gensane 1989; Stanic and Kennedy 1992; Stewart et al. 1994; Abraham 1997; Dunlop 1997; Lyons and Abraham 1999; Gallaudet and de Moustier 2003; Hellequin et al. 2003; Trevorrow 2004; Parnum et al. 2006; Siwabessy et al. 2006b). Those studies compared backscatter intensities from different seabed types on different incidence angle domains to theoretical distribution models such as Rayleigh, Rayleigh mixture, K , γ and log normal distributions. Stanic and Kennedy (1992) and Siwabessy et al. (2006b) observed in their data the log-normal distribution models for large incidence angles, whereas Lyons and Abraham (1999) observed K -distribution and Rayleigh mixture distribution models for all incidence angles. Lyons and Abraham (1999) and Gallaudet and de Moustier (2003), however, found that the backscatter statistics showed statistical distributions with heavier tails and multiple modes. In contrast, here we compare backscatter intensities at full incidence angles of a known seabed type to backscatter intensities at full incidence angles of all the other seabed types within the survey area.

The objective of this paper is to introduce a new technique to reliably predict “hard seabed” using a standalone application of a backscatter product, namely angular

backscatter response curves. We are aware of other methods using multiple predictive parameters derived from not only backscatter but also bathymetry, as reported in other studies (Huang et al. 2013, 2014; Li et al. 2013, 2016; Siwabessy et al. 2013; Daniell et al. 2015). The focus here is on demonstrating the utility of angular backscatter response as a dataset on its own.

Study area

Darwin Harbour is a tropical estuary formed within a drowned river valley, located on the northern coast of Australia (Fig. 1). The estuary comprises a main channel and three elongate arms: West Arm, Middle Arm and East Arm (Andutta et al. 2013). The Elizabeth River flows into East Arm, while the Darwin/Berry and Blackmore Rivers flow into Middle Arm. West Arm is without a prominent river. Subtidal areas of Middle Arm and East Arm are characterised by meandering channels, mid-channel sand bars and reefs, with intertidal areas occupied by broad flats, sand banks, reefs and mangrove forest (Fortune 2006; Smit et al. 2012). Within these two arms, it is estimated that within the open water areas (non-mangrove

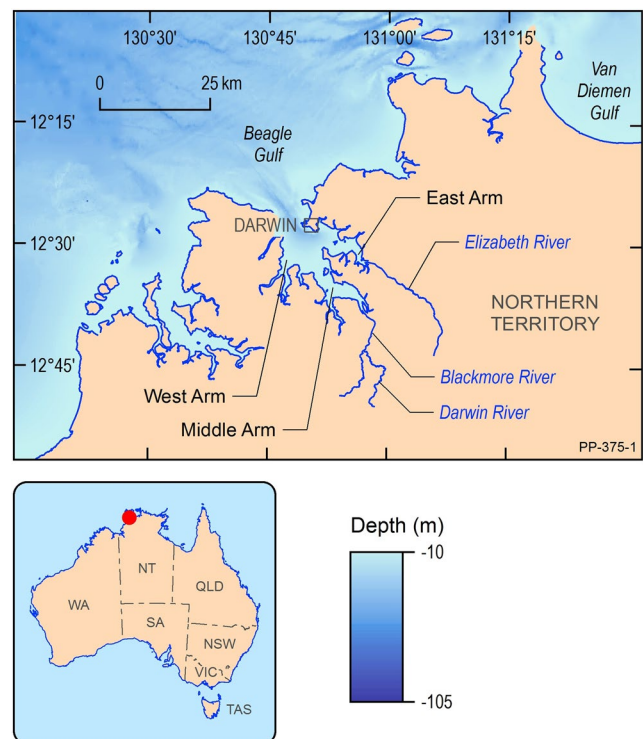


Fig. 1 General overview of the geographic settings of study area. The bathymetry grid is derived from ETOPO2v2 (National Geophysical Data Center 2006)

environment), subtidal and intertidal mobile sediments are the dominant substrate (45 and 37%, respectively); subtidal reefs are more extensive than intertidal reefs (10 and 2%, respectively) and within the non-photosynthetic zone, hard substrates occupy over a third of the available substrate (38%) (Smit et al. 2012). The seabed morphology of the main harbour area is dominated by a large channel and adjacent shore platforms and subtidal flats (Siwabessy et al. 2015). Between Mandorah and East Point, at the boundary between the outer harbour and the inner harbour, the main channel is up to 37 m deep (Figs. 2, 11). Maximum water depths are 27, 32 and 24 m in the West, Middle and East Arms, respectively. Channel widths range from 0.1 km in the Arms to ~1.2 km in the central channel. The nearshore habitats and coastline are predominantly sandy beaches with rocky headlands and sand flats with fringing rocky reefs.

The Darwin coastal region is macrotidal, having a maximum tidal range of 7.8 m, and mean spring and neap tidal ranges of 5.5 and 1.9 m, respectively (Woodroffe et al. 1988; Andutta et al. 2013). Tides dominate sediment transport, with tidal currents up to 2.5 m s^{-1} , while the effects of wind-driven currents, waves and river discharge appear negligible for sediment movement (Andutta et al. 2013). Turbid plumes can extend over wide areas of the harbour.

In middle Darwin Harbour, the main channel incises two adjacent Proterozoic bedrock units, the Welltree Metamorphics (gneiss) on the western side and the Burrell Creek Formation (shale, siltstone, sandstone) on the east (Northern Territory Geological Survey 1988). These are, in turn, overlain by Cretaceous sediments (clayey sandstone, sandy claystone, siltstone) of the Darwin Member of the Bathurst Island Group. Locally, these rocks variously form the headlands, shore platforms and reefs within and around Darwin Harbour.

Methods

Multibeam data acquisition and processing

Data for this study were collected during two surveys: a multibeam mapping survey and a sampling survey. The multibeam survey was undertaken between 24 June and 20 August 2011 on board the *M.V. Matthew Flinders* (iXSurvey 2011). A Kongsberg EM3002D 300 kHz multibeam sonar system was used to acquire high-resolution multibeam bathymetry and backscatter data across Darwin Harbour. Multibeam data were recorded using Kongsberg's Seabed Information System (SIS) software. Motion referencing and navigation data were collected with an Applix Position and Orientation system and a C-Nav GPS system (with a horizontal accuracy greater than $\pm 0.15 \text{ m}$) (for

more detail refer to iXSurvey 2011). Multibeam bathymetry data were processed using CARIS HIPS/SIPS v7.1 SP1 software. The processing steps included: the application of algorithms that corrected for tide and vessel pitch, roll and heave and; the use of software filters and a visual inspection of each swath line to remove any remaining artefacts and noisy data (e.g. nadir noise and data outliers). To minimise tidal bursts, a co-tidal solution in Caris™ was used. A high-resolution bathymetry surface (1 m horizontal resolution and a centimetre vertical resolution) relative to the Mean Sea Level (MSL) was created within Caris™ and then exported as an elevation grid (bathymetric map) for analysis.

Multibeam backscatter data were processed using the CMST-GA MB Process v10.10.17.0 toolbox software co-developed by the Centre for Marine Science and Technology (CMST) at Curtin University and Geoscience Australia (described in Gavrilov et al. 2005a, b; Parnum 2007) on the National Computational Infrastructure (NCI) supercomputer at the Australian National University. The processing steps included: removal of the system transmission loss; removal of the Kongsberg's specific angular dependence correction model; calculation of the angle of incidence; correction of the beam pattern; calculation of the angular backscatter response within a sliding window of 100 pings and; removal of the angular dependence and restoration to the backscatter strength at an angle of 40° (Gavrilov et al. 2005a, b; Parnum 2007; Gavrilov and Parnum 2010). Two processed backscatter datasets were then generated: a backscatter mosaic gridded from the backscatter energy to 1 m horizontal resolution and a set of angular backscatter response curves.

At 40° incidence angle or any incidence angles between 30° and 50° , discrimination across substrate types is the largest (Kloser et al. 2010; Lamarche et al. 2010; Kloser and Keith 2013). Based on the APL model (APL 1994), the dynamic range of seabed backscatter at 30 kHz for both consolidated and unconsolidated sediment at 40° incidence angle is 22 dB (Kloser and Keith 2013). The toolbox calculates two types of surface backscatter coefficients: backscatter intensity derived from the maximum backscatter envelopes, and; backscatter energy derived from the integral of the squared backscatter envelopes. We used the backscatter energy as recommended in Gavrilov and Parnum (2010) and Parnum and Gavrilov (2011). The surface backscatter coefficient estimated from the backscatter energy is robust concerning the effects of insonification area and beam pattern, and is comparable to instantaneous intensity (Gavrilov and Parnum 2010). In contrast, the surface backscatter coefficient estimated from the backscatter intensity leads to overestimation of the backscatter strength at large incidence angles of the outer beams when the footprint is much larger than the insonification area (Parnum and Gavrilov

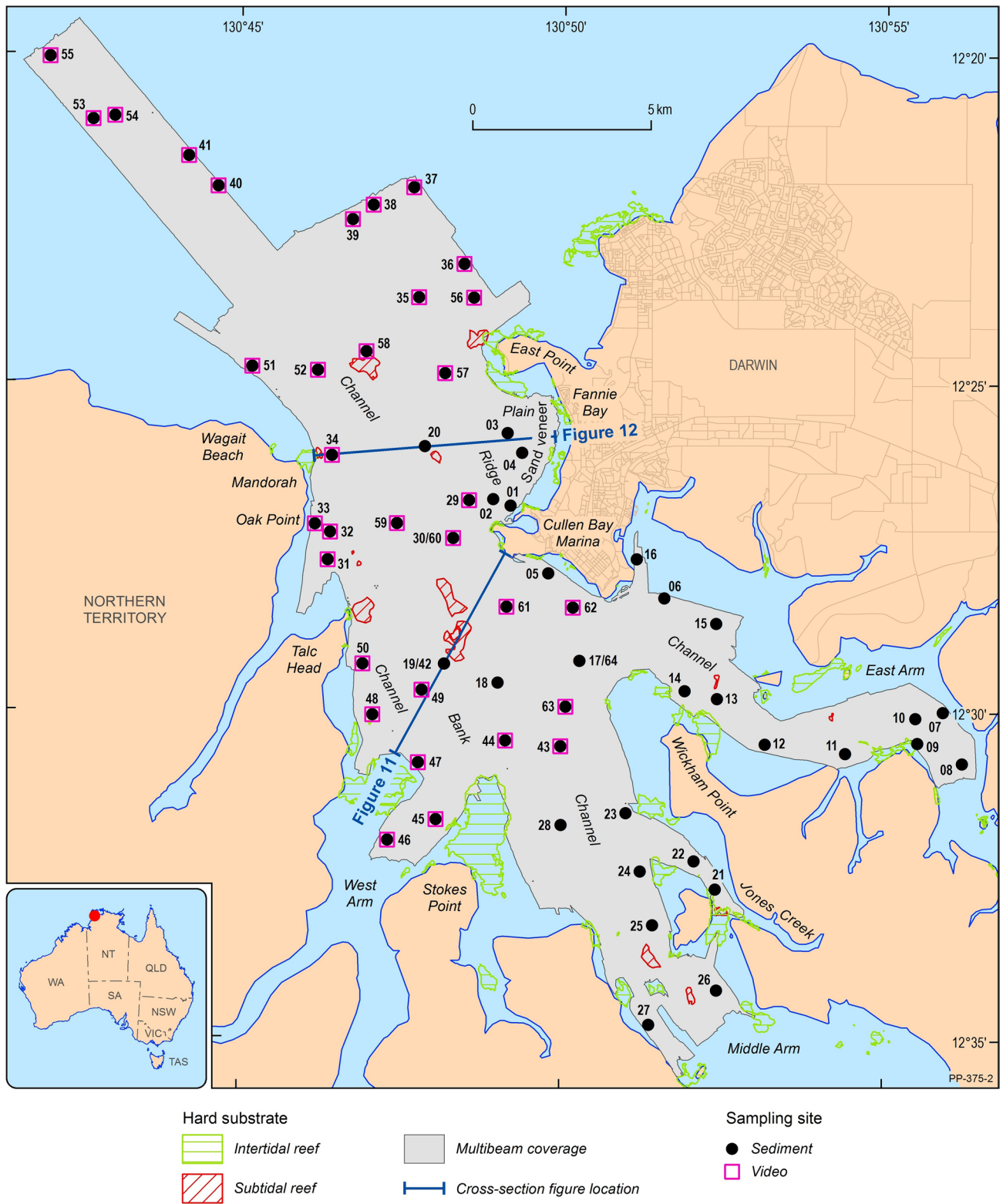


Fig. 2 Location map showing the multibeam coverage (grey) and the sample station numbers. Data supplied from DLRM is indicated in hashed polygons on figure (e.g. intertidal and subtidal reef outlines)

2011). Both estimates produced by the toolbox reduce the backscatter measurement to one surface backscatter coefficient per beam. Other backscatter processing software such as Geocoder maintain the full record of the backscatter measurements. Although the latter provides higher resolution of the backscatter scatter mosaic than the former, it doesn't significantly improve the classification results for shallow water multibeam systems in comparison to the effort allocated to produce such high resolution backscatter images. However, it does improve results for deep water multibeam systems as the across track distance between adjacent beams is large.

Angular backscatter response curves were calculated using a sliding window during the removal of the angular dependence from the backscatter to produce a consistent backscatter image across the swath for various incidence angles for a homogeneous seafloor. The sliding window approach was based on a 50% overlap in a 1° bin of incidence angle (Gavrilov et al. 2005a, b; Parnum 2007). Each angular backscatter response curve thus represents the average within the sliding window of 100 pings for each half-swath width. Based on our experience with our shallow water multibeam system, the 100 ping average improves the signal to noise ratio within a reasonable along track distance. The idea is to provide robust statistics within an optimum along track distance so that the along track homogeneity can reasonably hold. The length of the 100 ping average varies between 10 and 40 m depending on the survey speed and water depth. We calibrated the angular backscatter curves using sediment grain-size data and underwater video observations at stations where the derived bathymetry indicated a flat and sand-covered seabed. For each of these stations, an angular backscatter response curve was derived from the grain-size data using the APL seabed scattering model (APL 1994) and used to remove any residuals observed in the measured curves.

Seabed sample acquisition and processing

The seabed sampling survey, which included sediment sampling and underwater video capture, was undertaken between 17 and 22 June 2013 on board the *M.V. John Hickman* (Fig. 2). Sediment samples were collected using Van-Veen and Shipek sediment grabs. Video footage of the seabed at most sampling locations was obtained simultaneously using a real-time underwater video camera system mounted on the grab sample wire. The sampling locations were selected using a randomly stratified design based on backscatter values and depth range. The unsupervised ISO Clustering technique was used to divide the study area into five seabed classes based on the backscatter mosaic at the incidence angle of 40° and the bathymetry data. As a result, the five seabed classes which have distinct backscatter and

bathymetry characteristics can be assumed to represent different habitat types. Between 6 and 14 sites were then randomly selected from each of these five seabed classes across the study area as the sampling locations for the collection of sediment and video data. Sediment samples were analysed in Geoscience Australia's laboratory to produce sieve grain-size and laser grain-size distributions, and calcium carbonate content.

Seabed video analysis adopted a similar method to that described in Buhl-Mortensen and Buhl-Mortensen (2004) and Li et al. (2013), to characterise the local-scale sediment type and geomorphology. Continuous video footage was characterised for seabed substrate type and morphology (e.g. bedform and relief) based on 15 s sequences at 30 s intervals along each transect. Substrate type (e.g. boulder, cobble, pebble, granules, sand, and mud) was estimated as percentage cover to a precision of 10% (0, 10, 20...100%) using the Wentworth scale (Wentworth 1922) and geomorphology was defined as local "vertical relief" [e.g. flat (0–0.3 m), low (0.3–1 m), moderate (1–3 m)] and "bedform" type (e.g. ripples, waves, bioturbation) following Anderson et al. (2007). Substrate type was further modified based on the presence of sessile biota. Thus, if a majority of the 15 s footage sequence appeared to contain soft sediment, but the seabed supported biological entities that require hard substratum to grow, then the proportion of sediment covered with biota was classified as a sediment "vener". A qualitative assessment of substrate hardness (i.e. "hard" and "soft") was also derived from the seabed video footage and used to validate continuous multibeam data at a local scale. Thus, the hard seabed class was defined if rock, boulders, cobbles, pebbles, granules and/or "vener" were identified in either primary or secondary substrate types, whereas the "soft" class was identified if sand and mud was found in both primary and secondary substrate types.

Data integration: probability of hard seabed

The angular backscatter response curve data were analysed against the "hard" class derived from the seabed video characterisations to produce a dataset that indicated areas of "hard" seabed. The resulting curves from three training sites were consolidated into an "average curve", which became a reference curve of "hard" seabed. The average curve was compared to all other angular backscatter response curves using the Kolmogorov–Smirnov goodness of fit test to estimate the probability of the "hard" seabed (p -hard) and to test the null hypothesis at $\alpha=0.05$ (H_0 : all other angular backscatter response curves \geq the reference angular backscatter response curve). "Mixed patches" become irrelevant here for a binary class solution because they will be allocated to either "hard" seabed class or not,

depending on the proportion of “hard” seabed that contributes to the average angular backscatter response curve of the patch. Finally, the Inverse Distance Weighted and Nearest Neighbour interpolation techniques were used to produce continuous layers of the p -hard and derived hard seabed parameters for the mapped area of Darwin Harbour, respectively.

Accuracy assessment

The accuracy assessment for seabed mapping was conducted on the reference data taken from the original dataset that has not been used as training data, following Diesing et al. (2016). The performance of the prediction map was assessed using the overall accuracy, and producer’s and user’s accuracies derived from a confusion matrix, also known as a contingency table (Congalton 1991). The confusion matrix contains a tally of agreement between predicted and reference data at test sample sites, excluding the three training sites. The producer’s accuracy is a measure of omission error, indicating the probability of a reference (ground) sample being correctly classified. The user’s accuracy is a measure of commission error and is indicative of the probability that a sample from the classified map correctly represents that category on the ground. The overall accuracy is the percentage of the ground samples being correctly classified.

As it is advisable to provide other measures of accuracy in addition to the confusion matrix (Stephens and Diesing 2014; Diesing et al. 2016), we used the area under curve (AUC) statistic (Fielding and Bell 1997) at test sample sites, excluding the three training sites. The AUC is independent of prevalence of the classes in the samples (Bradley 1997) and thus is often used to assess the performance of binary prediction. The AUC is estimated from the receiver operating characteristic (ROC) plot, showing the true positive fractions as a function of their false positive fractions. The value varies from 0 to 1 with a value of 0.5 indicating the prediction is no better than random; a value of 0.7 indicating 70% of the time a random section from the positive group will have a score greater than the negative group; and a value of 1 indicating perfect discrimination.

Bed shear stress

Tidal currents have been measured previously at many locations in Darwin Harbour to calibrate and verify a detailed hydrodynamic model (Williams et al. 2006). Here we use outputs of that model to calculate the bed shear stress over the harbour domain using the RMA suite of numerical hydrodynamic models for estuaries (King 2016). The shear stress data were used to indicate where in the area mapped it was likely that sediment on the seabed was mobile. This

information helps identify areas that may be intermittently covered by sediment or scoured down to bedrock.

Results

Seabed morphology

A total of 178 km² of multibeam bathymetry data was acquired, showing that the seafloor of Darwin Harbour is complex and irregular with water depths varying between 1 and 43 m (relative to MSL; Fig. 3). Primary geomorphic features include channels, banks, ridges and plains. The predominant feature of the area is a 40 m deep mid-harbour channel that splits into narrower and shallower (9–20 m deep) channels. These channels are flanked by plains (3–5 m water depth) that extend to the intertidal zone and near shore of Cullen Bay and Fannie Bay. Ridges and banks form localised shoals that rise to less than 3 m water depth, such as in outer Fannie Bay, west of the harbour channel entrance and in between West and Middle Arms, and have typically steep flanks and walls (10°). The mid-harbour and Middle Arm channels and the ridge near Fannie Bay display a more rugged seabed than shallow plain areas that are typically flat.

Multibeam backscatter

Backscatter strength ranged between -1 and -63 dB (Fig. 4). High backscatter is typically associated with raised seabed features, such as banks and ridges, while lower backscatter is associated with soft sediments mostly within channels, depressions and plains (Figs. 4, 5). This contrast is well illustrated by the sandy plain area within Cullen Bay and Fannie Bay where backscatter strength is low (mean ~ -27 dB), and the ridge to the west where backscatter is much higher (mean ~ -8 dB). Similarly, areas of shallow reef and a large bank at the central western end of the Harbour have high backscatter strength (mean ~ -15 dB).

The angular backscatter response for the Darwin Harbour dataset is summarised in a density plot that represents 219,518 response curves (Fig. 6). The density plot shows a significant range in the response curves of approximately 20 dB across the range of incidence angles with a maximum angular response of 69° for each side of the swath.

Underwater video characterisations

Seabed video characterisations correlated with backscatter strength and p -hard but are not strongly correlated with bathymetry (Fig. 7). Results from t test statistics suggested that the mean backscatter of the two video classes is significantly different at $\alpha=0.01$ ($p=0.0044$). Similarly, the

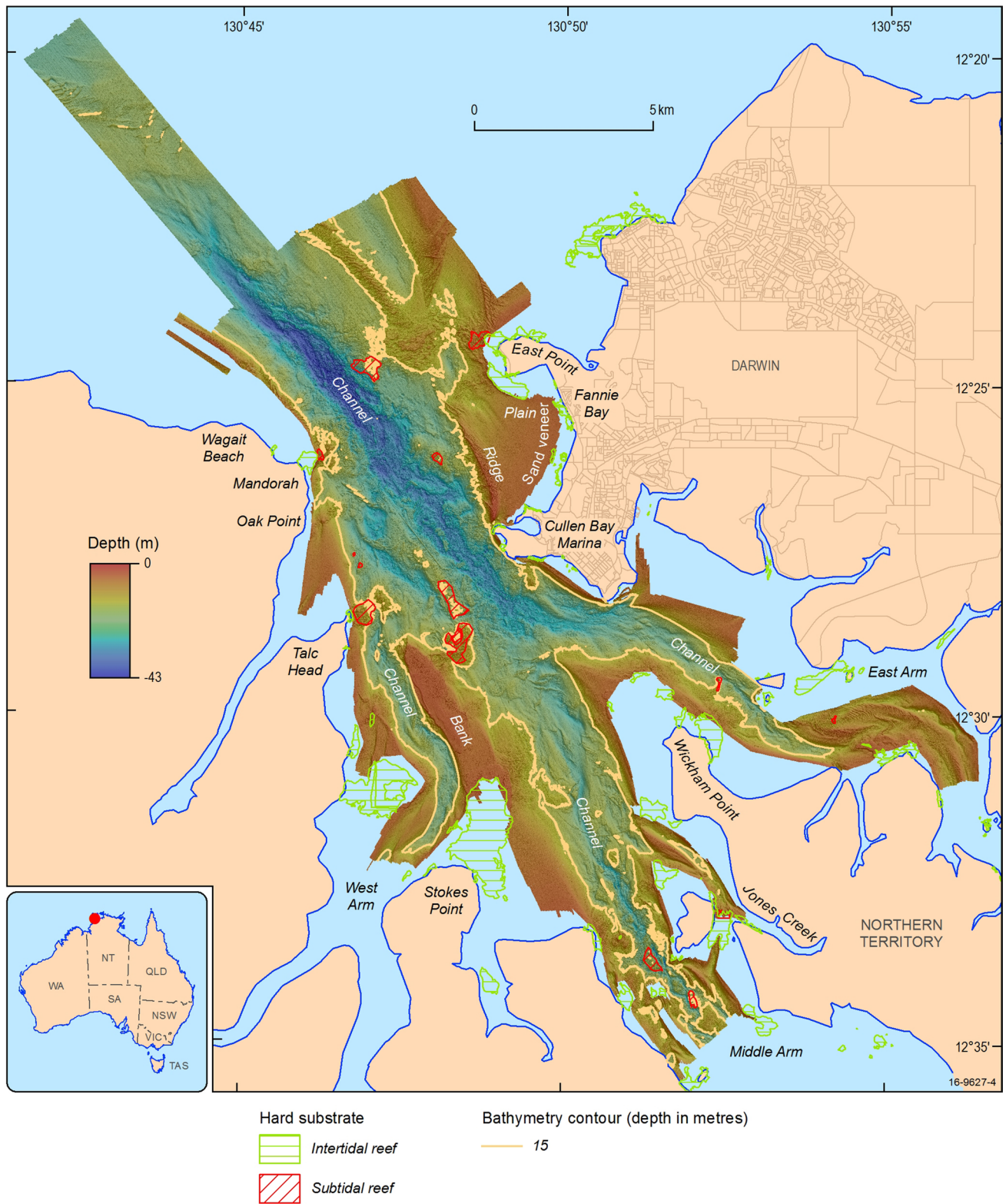


Fig. 3 False colour hillshaded bathymetry image (45° azimuth, 45° altitude and 70% transparency) with representative examples of main geomorphic features overlaid with intertidal and subtidal hard substrate, and a 15 m depth contour

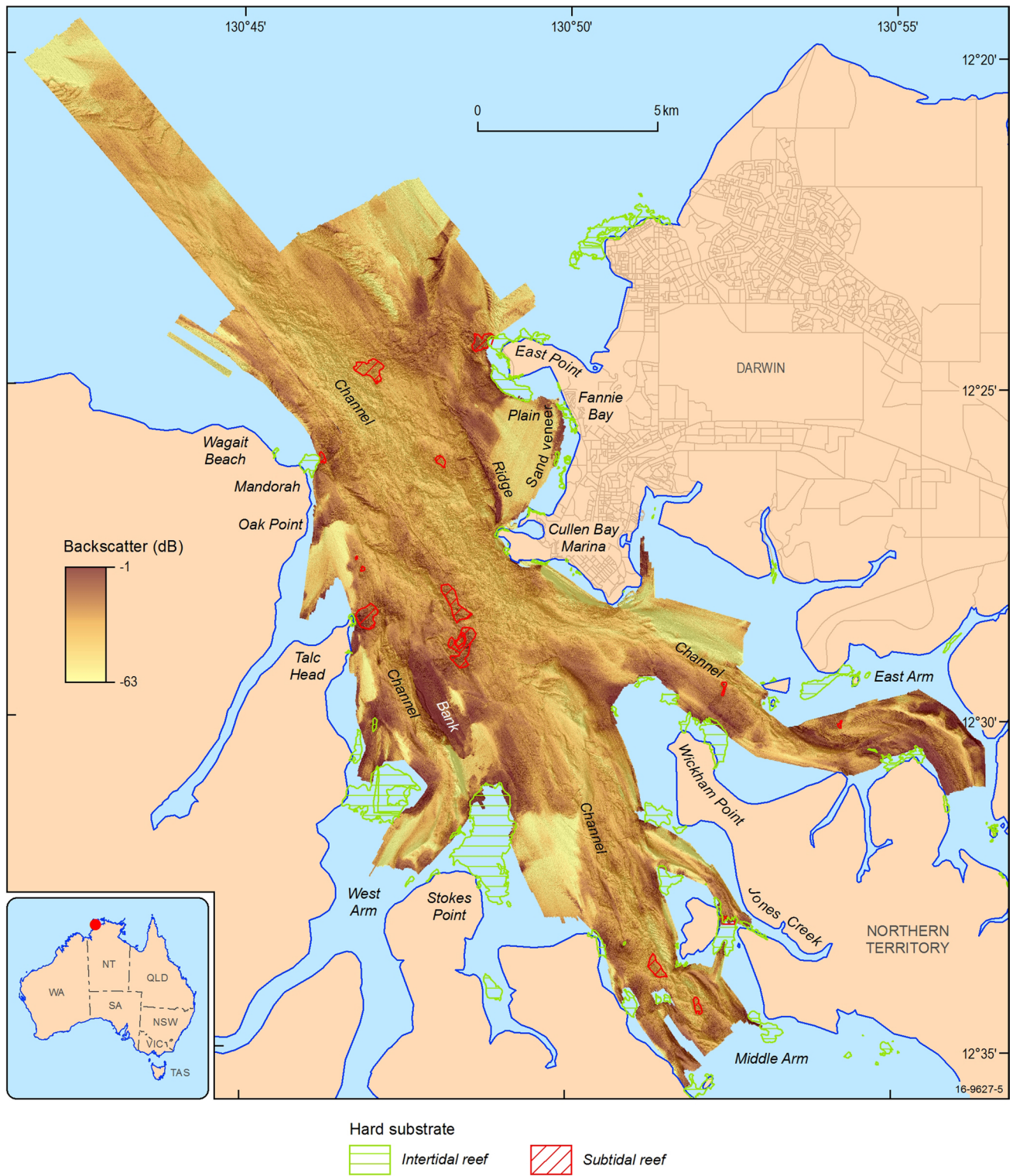


Fig. 4 False colour backscatter image overlaid with intertidal and subtidal hard substrate and a hillshade bathymetry (as per Fig. 3)

p-hard of the video categories is significantly different at $\alpha=0.01$ ($p=0.0021$). In contrast, the depth of the two video categories is not significantly different ($p=0.8338$).

The *p*-hard has the lowest probability indicating that the two video categories are well discriminated by the *p*-hard. Soft seabed substrates were recorded in areas of low

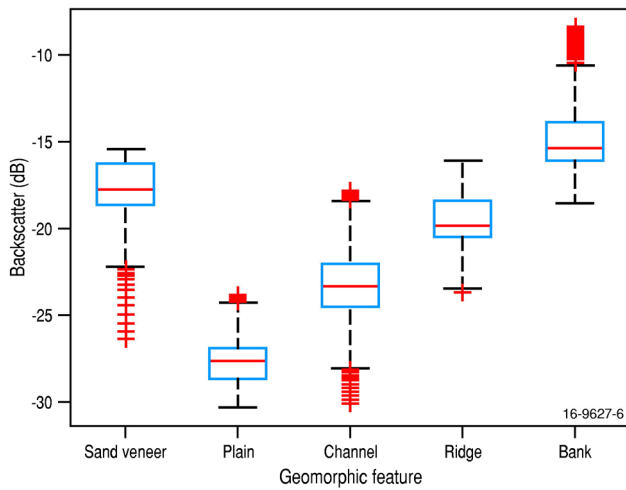


Fig. 5 Boxplot of backscatter strength in relation to the representative examples of geomorphic features highlighted in Fig. 4. The backscatter values were extracted from representative areas of the geomorphic feature (as labelled in Fig. 4) and various statistics such as median (red line), interquartile range spanning from 1st quartile to 3rd quartile (blue box) and whiskers showing minimum and maximum (black tick) were calculated to form the boxplot

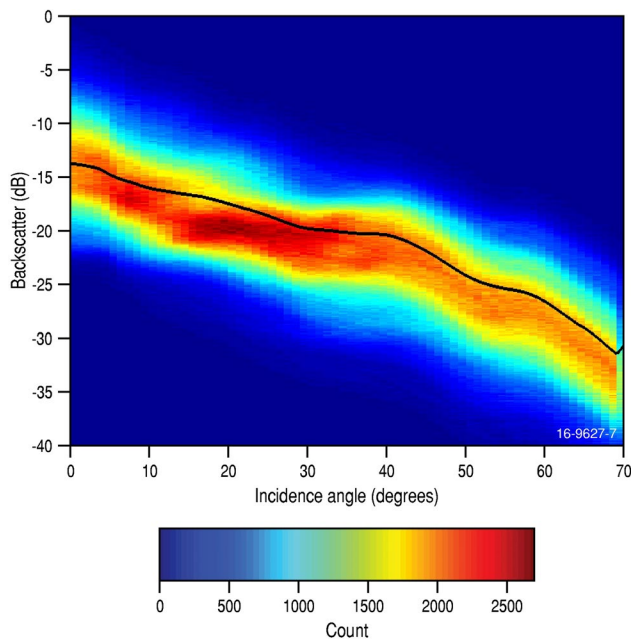


Fig. 6 Density plot of angular backscatter response of the Darwin Harbour seabed. Overlaid on the density map is the reference angular backscatter response curve representative of “hard” seabed (black line)

backscatter strength such as plains and channels, while hard seabed substrates occurred in areas of high backscatter strength, such as banks, ridges and more rugged seabed features. However, there were some discrepancies between the video characterisation, backscatter strength

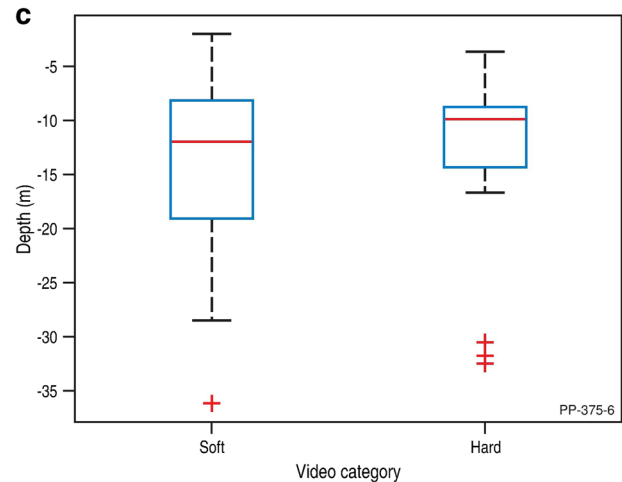
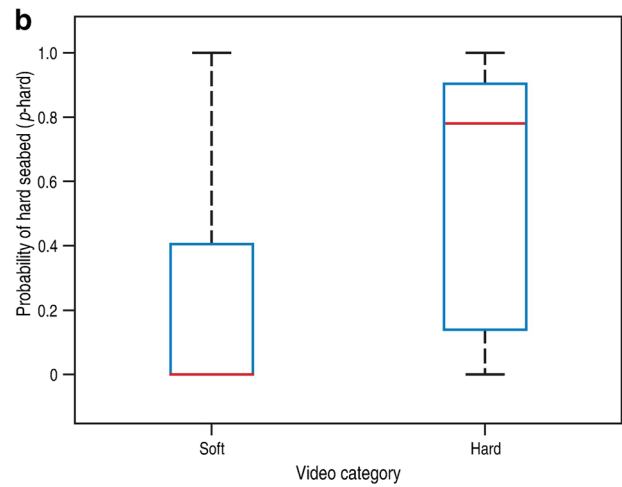
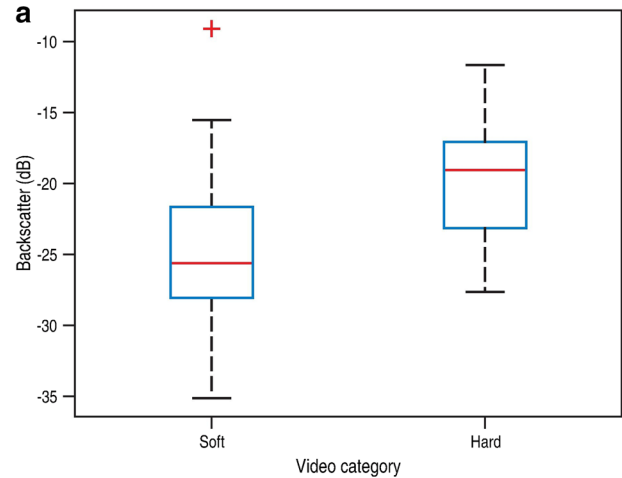


Fig. 7 Boxplots. **a** Backscatter strength grouped into seabed video categories, **b** probability of hard seabed (p -hard) grouped into seabed video categories, and **c** depth grouped into seabed video categories. The mean backscatter of the video categories is significantly different based on t test statistics at $\alpha=0.01$ ($p=0.0044$) and similarly the p -hard of the video categories ($p=0.0021$). However, the two video categories are not different for depth ($p=0.83$)

and grain-size composition at some locations. For example, three stations located in the main channel were classified as dominantly hard seabed based on the epifaunal biota such

as large barrel sponges and dense gorgonian beds observed in video footage, but recorded low backscatter strength and high mud composition for the other datasets. These

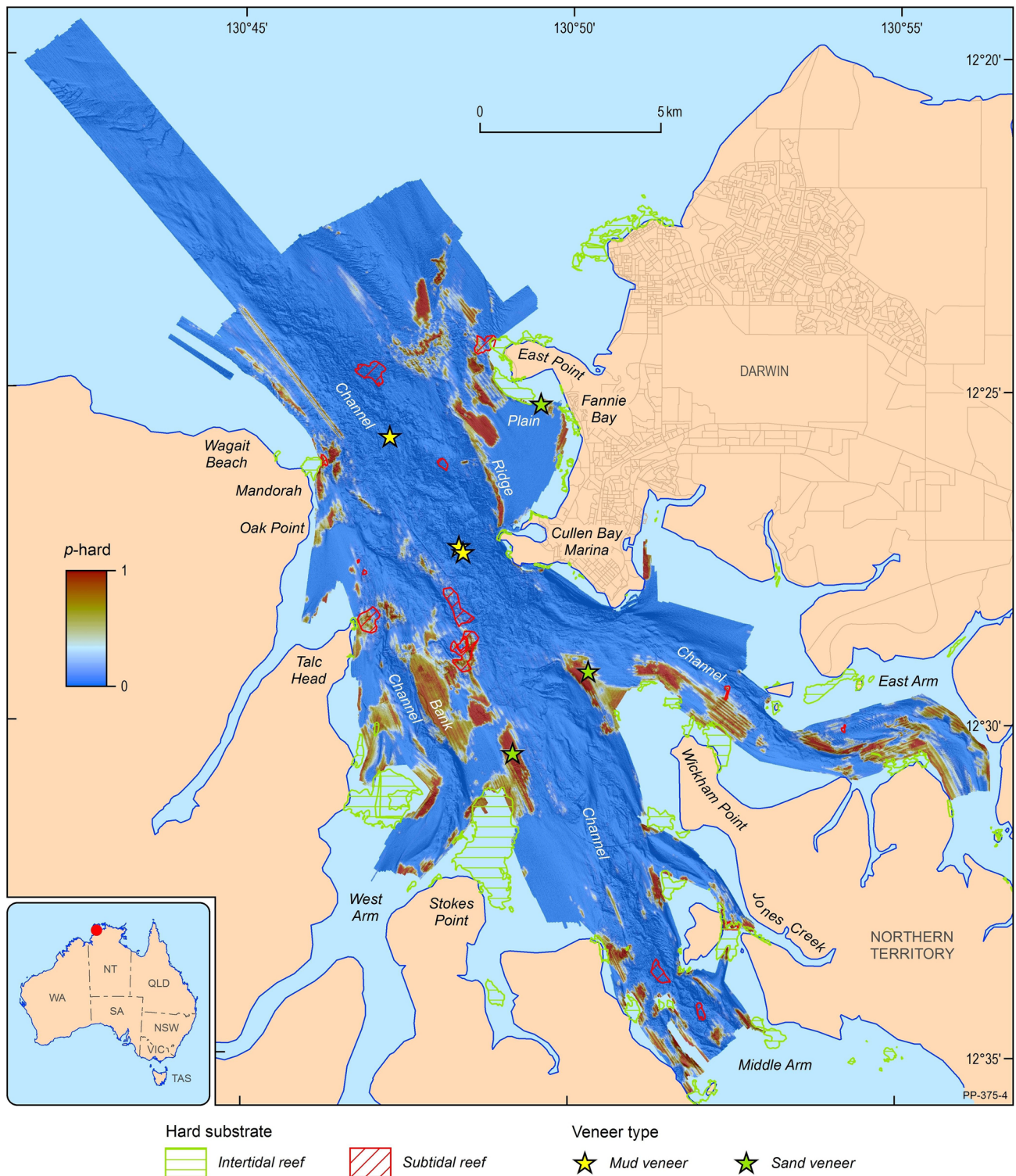


Fig. 8 False colour probability of hard substrate (p -hard parameter) for Darwin Harbour seabed overlaid with a hillshade bathymetry (as per Fig. 3)

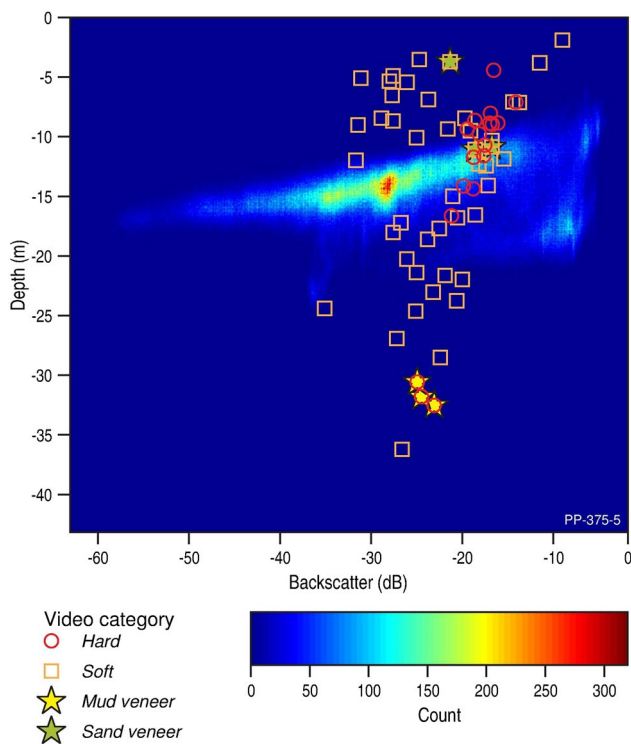


Fig. 9 Density plot of backscatter versus depth. Overlaid on the density map is the video category

sites were therefore classified as “mud veneer” (Figs. 8, 9) within 30–35 m water depth and backscatter less than -22 dB (Fig. 9). Conversely, soft-dominated seabed types were associated with high backscatter strength and high sand composition at several sites (e.g. the plains in Fannie Bay, between East and Middle Arms, and between Middle and West Arms) (Figs. 8, 9). These areas were therefore classified as “sand veneer”.

Probability of hard seabed and derived hard substrate maps

Areas of high probability of hard seabed (p -hard) and predicted hard seabed as derived from the null hypothesis H_0 test in Darwin Harbour are patchy and localised to narrow areas alongside channels and on banks and ridges (Figs. 8, 10). They occupy a total area of 41 km^2 , which represents 23% of the total area mapped (Fig. 10). Bathymetric cross-sections of the harbour, both in the central region and towards the mouth, confirm that high p -hard values are generally associated with banks, ridges and other elevated geomorphic features as well as the sand-veneered seabed identified within the shallow sandy plain (Figs. 11, 12). The profiles also highlight the positive association between p -hard and high backscatter strength. Both backscatter products show a pipeline to the north of Wagait Beach,

but fail to show other known pipelines in the harbour. This likely indicates that these pipelines may have been buried by mobilised sediment or as they were laid.

The confusion matrix suggests that the overall classification accuracy is 75% and the producer’s accuracy for hard seabed is 79%, indicating a near 80% performance accuracy of the hard seabed reference data (Table 1). An additional assessment using the AUC suggests that the performance accuracy is 0.79, indicating that 79% of the time a random selection from the positive class have a score greater than a random selection from the negative class. The derived maps show that hard seabed predominantly occurs in five areas (Figs. 8, 10): between Stokes Point and Talc Head (34% of the total predicted hard seabed), Wickham Point to East Arm (25% of the total predicted hard seabed), between East Point and Cullen Bay (20% of the total predicted hard seabed), Middle Arm including Jones Creek (13% of the total predicted hard seabed) and Mandorah, between Oak Point and Wagait Beach (9% of the total predicted hard seabed).

Intertidal and subtidal hard seabed substrates were previously mapped by the Department of Land Resource Management (DLRM) of the Northern Territory Government (NTG) in 2011 and manually digitised from low-tide aerial photographs (Fig. 10) and are used here as an additional partial validation of the backscatter derived products. Of the 12.53 km^2 of intertidal area mapped from air photos, there was only 0.72 km^2 of overlap with the area mapped in this study. Within this overlap area there was 94% (0.68 km^2) agreement with the hard seabed map derived from angular backscatter response data. The subtidal hard seabed map was separately generated independently by DLRM using the benthic position index (Lundblad et al. 2006), rugosity and slope maps in combination with prior knowledge of the area (Smit et al. 2012). Of the total study area of 178 km^2 , only 2.02 km^2 (1%) is hard subtidal seabed. Of this, 55% ($\sim 1 \text{ km}^2$) coincides with the hard/rocky seabed map derived from backscatter data. Most disagreement occurs in the subtidal areas characterised by a “mud veneer” substrate.

Bed shear stress

The velocity of tidal currents in Darwin harbour is energetic with tidal flows of up to 2 m s^{-1} . However, tidal currents of this magnitude are short lived during a tidal cycle with a maximum duration of 1 h during spring tides. Tidal currents up to 1 m s^{-1} occur for up to 10% of the time for combined neap and spring tide ranges. Modelling of bed shear stress shows distinct variations across Darwin Harbour (Fig. 13) that relate to substrate types. Sand covered areas have bed shear stress values that exceed 0.1 N m^{-2} and of sufficient magnitude for sand transport (Van Rijn 2007). By

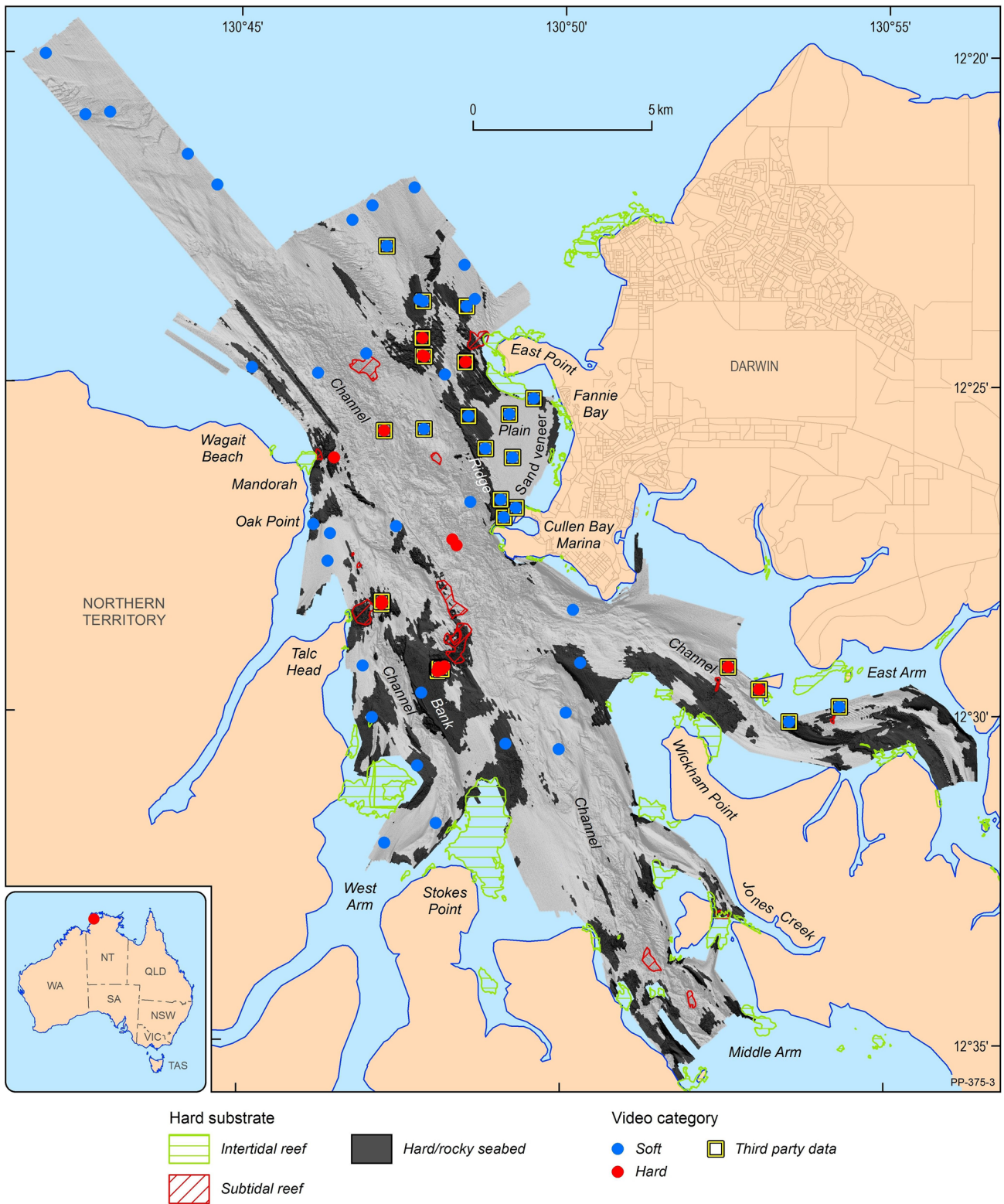
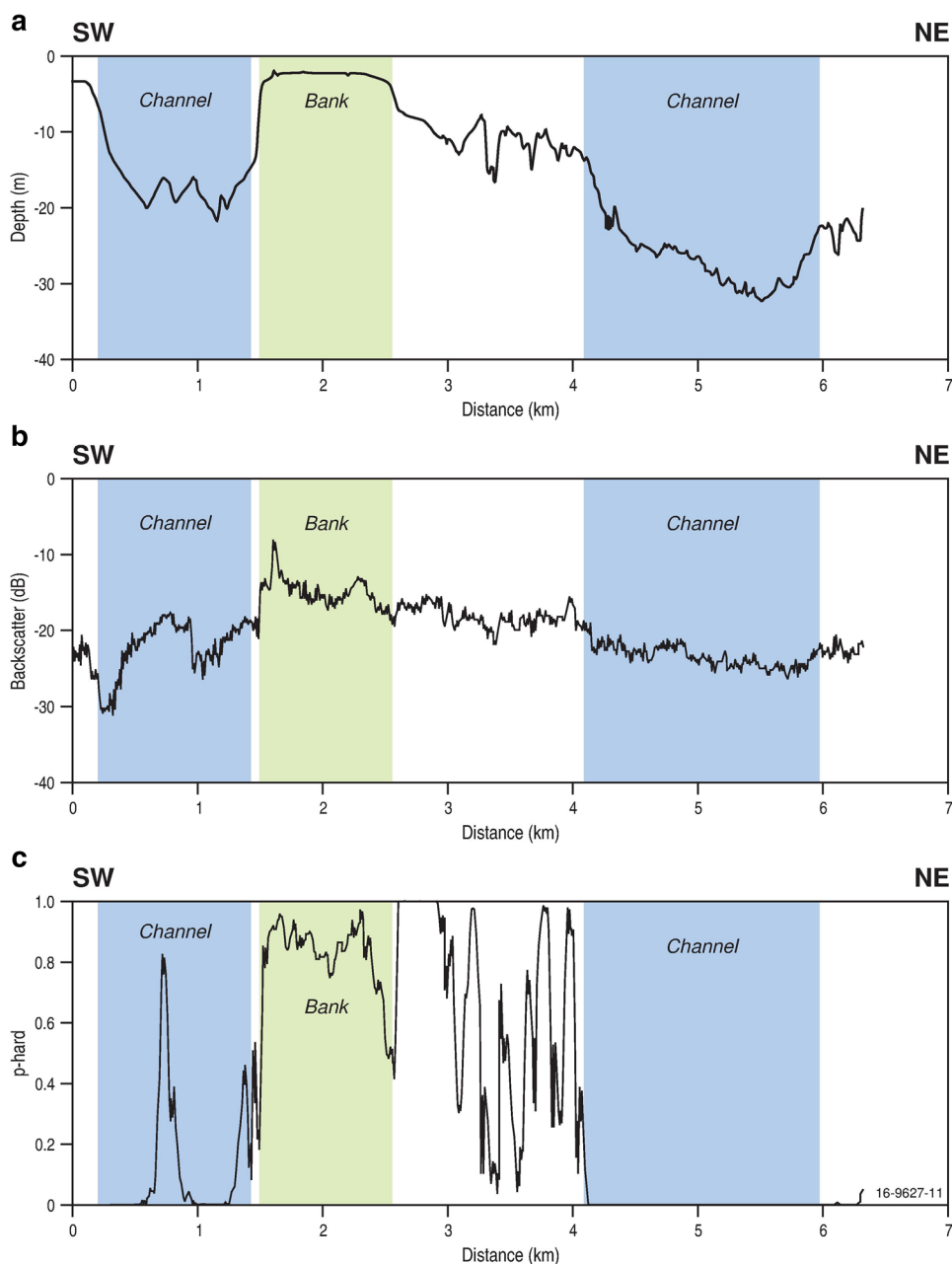


Fig. 10 “Hard” seabed map of the Darwin Harbour based on the null hypothesis H_0 test at significance level $\alpha=0.05$ overlaid with a hill-shaded bathymetry (as per Fig. 3). The hard substrate areas from Smit et al. (2012) are also shown

Fig. 11 **a** Water depth, **b** backscatter strength, and **c** *p*-hard profile for a cross-section of Darwin Harbour (see Fig. 2 for location) showing high backscatter values associated with a bank feature and lower values in channels



contrast, shear stress exceeds 0.4 N m^{-2} across known reefs and areas of very coarse sand. Similarly, shear stresses of $0.2\text{--}0.8 \text{ N m}^{-2}$ are modelled for the large sand bars in the middle of East Arm. Lower values of $0.03\text{--}0.1 \text{ N m}^{-2}$ for the intertidal mud flats, and between 0.001 and 0.05 N m^{-2} on fringing mangrove zones, indicate only silt would potentially be mobilised in these areas. Local variations in bed shear are also modelled, such as around the Cullen Bay sand bar where significant shear exists on one side of the bar (up to 1.0 N m^{-2}). This results in the deep drop off and

the diffusion of sand toward the bay to form the distinctive shape of the bar.

Discussion

Model performance and applications

The technique presented in this study is automated and faster than manual mapping techniques used to produce

Fig. 12 **a** Water depth, **b** backscatter strength, and **c** *p*-hard profile for a cross-section of outer Darwin Harbour (see Fig. 2 for location) showing high backscatter values associated with a ridge feature and thin sand veneer, and low backscatter values associated with a soft sandy plain

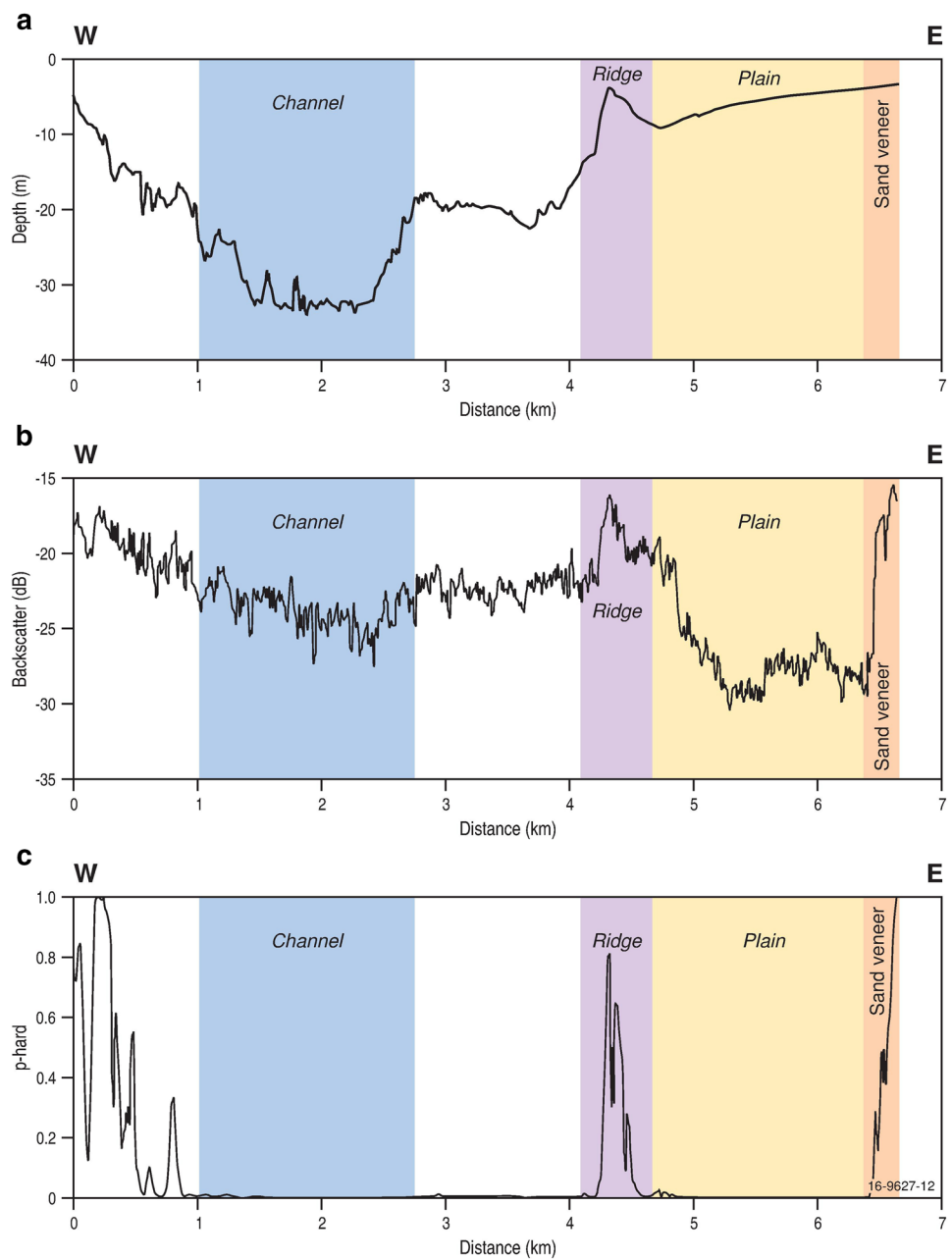


Table 1 Confusion matrix between classification map and ground-truth (video) data at test sample sites, excluding the three training sites

	Ground-truth (video)			User's acc.
	Soft	Hard/rocky	Total	
Classification				
Soft	31	1	32	0.89
Hard/rocky	14	15	29	0.52
Total	45	16	61	
Producer's acc.	0.69	0.79		
Overall accuracy				0.75

the previous intertidal and subtidal hard/rocky seabed layers of Darwin Harbour, which were time-consuming and relied on expert knowledge. Our results show that this automated approach is able to predict the distribution of hard seabed with relatively high levels of reliability (e.g. 94% agreement with existing seabed maps). This is particularly useful for informing the management of seabed environments such as Darwin Harbour that experience high levels of turbidity and very energetic tidal currents which restrict the application of more traditional benthic habitat mapping approaches. Importantly, mapping the likely distribution of hard seabed can be used to improve the planning of biological surveys and selection of monitoring sites by identifying

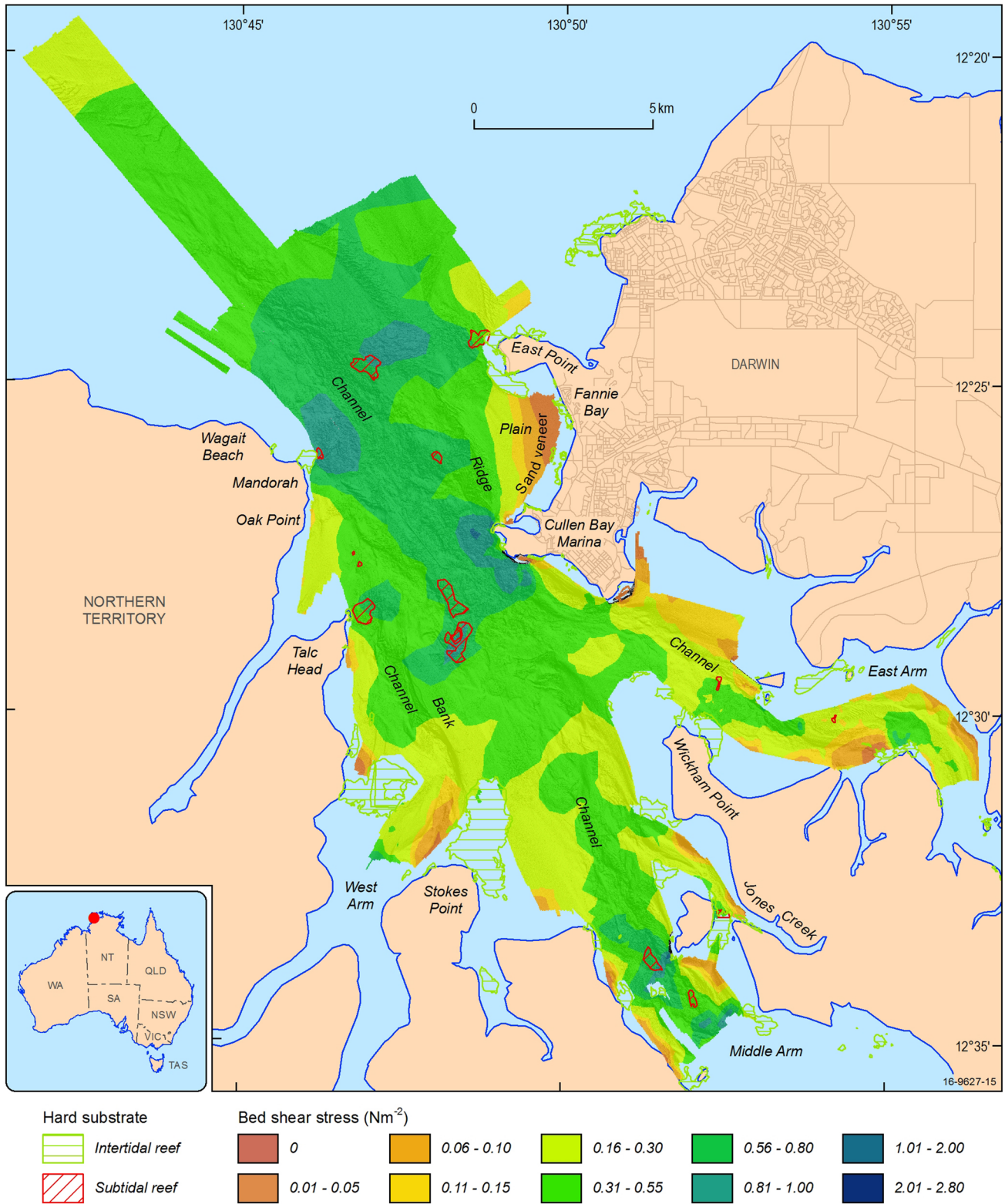


Fig. 13 Darwin Harbour seabed shear stress 75th percentile, derived from the hydrodynamic model of Williams et al. (2006) overlaid with a hillshaded bathymetry (as per Fig. 3)

areas that are potentially ecologically important. For example, coral communities comprised of hard scleractinian coral beds (e.g. *Symphyllia* and *Turbinaria* colonies) as well as non-scleractinian calcareous coral species (e.g. *Tubipora musica* and *Junceella fragilis* colonies) are generally limited in Darwin Harbour to depths of 10 m and sparsely distributed (Wolstenholme et al. 1997). Knowledge of the potential distribution of hardground habitat will allow for more effective management and monitoring of these important communities.

Angular backscatter response curves are increasingly being utilised in seabed classification and characterisation studies as they intrinsically represent seabed properties in greater angular resolution than backscatter mosaics can provide. This improved resolution in turn allows for better class separation than if a backscatter mosaic alone is used, as this information becomes lost when generating the mosaic for subsequent classification. The use of the response curves as a standalone parameter or together with other parameters is increasing in studies of complex seabeds (Hamilton and Parnum 2011; Huang et al. 2013, 2014; Li et al. 2013, 2016; Siwabessy et al. 2013; Daniell et al. 2015). In our previous study, *p*-hard is identified as the most important standalone predictive parameter for seabed hardness modelling in a turbid, macrotidal environment and is consistent with previous studies that have utilised this parameter in different types of marine environments (Li et al. 2013, 2016; Siwabessy et al. 2013). Siwabessy et al. (2013) introduced two different techniques for seabed classification; the use of angular backscatter response curves only, and multiple predictors (including *p*-hard). The use of angular response curves alone resulted in 78% overall classification accuracy in that study, which is comparable to the overall classification accuracy of the present study. However, when multiple predictors were introduced, the accuracy increased to 87%. In a similar study, a higher overall classification accuracy of 89% was obtained with the use of multiple predictors (including *p*-hard; Li et al. 2016). This highlights the importance of incorporating other predictors on increasing the overall accuracy for seabed classification.

Model limitations and uncertainties

Angular backscatter response curves are lower in spatial resolution than backscatter mosaics because they are generated by taking the average of a stack of backscatter strength values as a function of incidence angles within a sliding window. In addition, the assumption that the seabed is homogeneous across half of the multibeam swath, as adopted in this study, does not always hold. These uncertainties are propagated to the derived parameters, such as our *p*-hard and hard seabed map outputs. In addition, to produce a continuous surface map, these two backscatter

datasets require spatial interpolation, which also affects the accuracy of the map. However, this is countered somewhat by the densely spaced acoustic pings in this shallow water dataset.

The fact that the angular backscatter response curves were derived from individual sliding windows made it difficult to include textural measures into the seabed classification. Another particular constraint of this study was the limited sampling, including a lack of representative sediment and video samples from channels in the East and Middle Arms of Darwin Harbour. These reaches of the harbour include areas of relatively high bed shear stress (Fig. 13) and their morphology suggests that they have a high probability of being hard/rocky seabed, but this is yet to be validated by field observations. This may explain the low user's accuracies (e.g. 52%) obtained for the hard/rocky seabed type, and points to the utility of the shear-stress model for informing sampling strategies. Nevertheless, the actual prediction map does show that this new approach was able to predict hard/rocky seabed at locations elsewhere where they might be expected to occur.

The validation techniques used here (i.e. underwater video and sediment samples), were successful in delineating clear differences between habitat classes and highlighting areas of soft sediment veneer. Without these validation techniques, areas of veneer would have been misclassified as hard ground based on the backscatter response. However, these techniques provide little (if any) information about the sub-surface deeper than a few decimetres below the surface of the seabed. Penetration of the acoustic signal into sediments depends on sediment type, incidence angles and frequencies (Mitchell 1993; Hillman et al. 2017). This becomes more profound for low frequency systems than high frequency systems e.g. 5–30 m for 6.5–12 kHz systems and ~0.5–0.8 m for 100 kHz system in fined-grained sediments at 60° incidence angle (Mitchell 1993). Clearly, additional sampling or acoustic devices, such as seabed penetrometers or sub-bottom profilers, would further test the model outputs for areas of sediment veneer. The presence of a veneer of sediment over hard seabed and, at least episodically, within epifaunal habitat, is consistent with high levels of bed shear stress (e.g. $>0.3 \text{ N m}^{-2}$) throughout most of the area mapped (Fig. 13), which are capable of mobilising all the sediment types sampled (mud to coarse sand).

The discrepancy between the video and the acoustic classification results from Darwin Harbour may also relate to differences in the spatial scale of observations. That is, underwater video data (fine-scale point source at cm resolution) relative to continuously-acquired backscatter data (broad-scale at m resolution) may not always allow for coherent matching of habitat information particularly for fine-scale features detected in video that are simply not

resolved in multibeam acoustic data. Additionally, hard-packed/consolidated sediment may result in higher backscatter returns, but may not be able to support epifauna, and would therefore not be classed as a “vener”. It is the hard, shallow sub-bottom underneath a few decimetres or less of sand that returns a high backscatter signal. This becomes a problem where there is no sessile biota observed and the video data fail to distinguish the presence of “sand veneer”. Overall, however, the results are consistent with the current state of knowledge on geoacoustics, namely, that most acoustically hard substrates are dominated by hard sediments and rock, whereas most acoustically soft substrates are associated with soft, finer-grained sediments.

The sampling design used in this study was randomly stratified based on backscatter values and depth range. However, for calibrated multibeam systems, it is useful to also generate a predicted p -hard layer based on the theoretical angular backscatter response curve for the “pebbles” sediment class as the minimum threshold for detecting hard substrate. This would more specifically target the potential p -hard layer and capture some of the classification uncertainties, such as “vener” classes. As discussed previously, “mud veneer” (hard video class, low backscatter strength) or “sand veneer” and areas of hard-packed sediments (soft video class, high backscatter strength) are the most problematic areas to model accurately. To better capture these areas and increase the robustness of the model, we recommend that in future studies, the sampling design also take into consideration manually selected areas based on the morphological characteristics of the seabed. For example, veneers are likely to be located adjacent to hard non-veneer areas and show a relatively smooth surface. In any case, sampling some areas based on their morphology may help resolve the backscatter signals of certain seabed features, such as hard pavement. Finally, in the present study, only sand sediment samples were used to calibrate the angular backscatter response curves. The model robustness could be potentially increased by using all sediment samples across the textural range (mud, sand, gravel).

Conclusion

This study demonstrates the value of multibeam acoustic data to objectively predict the spatial distribution of seabed hardness over large areas. Angular backscatter response data provide significantly more information than single normalised backscatter values. Importantly, utilising the full angular backscatter response preserves the acoustic properties of the seabed and can successfully delineate hard from soft seabed. This is a particularly important technique in high-turbidity, high-current settings such as Darwin Harbour, where the application of diver surveys and satellite

and aerial remote sensing techniques can be very limited and costly.

This study confirms the strong positive relationship between backscatter strength, angular backscatter response and seabed hardness, whereby acoustically hard areas are dominated by hard/rocky seabed and relatively coarse sediments, and acoustically soft seabed dominantly comprise soft and muddy sediments. Importantly, the p -hard and hard/rocky seabed maps describe key physical environmental characteristics of the harbour that can be used to predictively model biodiversity, indicate the potential locations of biologically important areas, and usefully inform subsequent surveys that aim to target a range of benthic habitats and biological communities.

Acknowledgements This study was undertaken by Geoscience Australia (GA) and the Department of Environment and Natural Resources’ predecessor, the Department of Land Resource Management (DLRM) of the Northern Territory Government (NTG) and funded by NTG with co-investment by GA, Australian Institute of Marine Science (AIMS) and Darwin Port Corporation. We thank the master and crews of *M.V. Matthew Flinders* and *M.V. John Hickman* for their support in conducting successful surveys in 2011 and 2013, respectively; Mark Matthews of iXSurvey Australia Pty Ltd for conducting the multibeam survey in 2011; the Field and Engineering Support staff at GA for logistical support prior to the multibeam survey in 2011 and involvement in the physical sampling survey in 2013; and Dr. Tony Griffiths of DLRM for support during the physical sampling survey in 2013. Sediment samples were analysed by the Palaeontology and Sedimentology Laboratory, GA. We acknowledge the National Computational Infrastructure at the Australian National University for provision of world-class computing resources. Reviews by Dr. Andrew Carroll and Dr. Johnathan Kool (GA) and two anonymous reviewers helped to significantly improve the paper. This work is published with permission of the Chief Executive Officer, Geoscience Australia.

Open Access This article is distributed under the terms of the Creative Commons Attribution 4.0 International License (<http://creativecommons.org/licenses/by/4.0/>), which permits unrestricted use, distribution, and reproduction in any medium, provided you give appropriate credit to the original author(s) and the source, provide a link to the Creative Commons license, and indicate if changes were made.

References

- Abraham DA (1997) Modelling non-Rayleigh reverberation. SACLANT Undersea Research Centre Report. SACLANTCEN SR-266
- Anderson TJ, Cochrane GR, Roberts DA, Chezard H, Hatcher G (2007) A rapid method to characterize seabed habitats and associated macro-organisms. In: Todd BJ, Green HG (eds) Mapping the seafloor for habitat characterization, vol 47. Geological Association of Canada, St. John’s, pp 71–79
- Andutta FP, Wang XH, Li L, Williams D (2013) Hydrodynamics and sediment transport in a macro-tidal estuary: Darwin Harbour, Australia. In: Wolanski E (ed) Estuaries of Australia in 2050 and beyond. Springer, Dordrecht

- APL (1994) APL-UW high-frequency ocean environment acoustic models handbook (APL-UW TR9407). Applied Physics Laboratory, University of Washington, Seattle
- Banks KW, Riegl BM, Richards VP, Walker BK, Helme KP, Jordan LKB, Phipps J, Shivji MS, Speiler RE, Dodge RE (2008) The reef tract of continental southeast Florida (Miami-Dade, Broward and Palm Beach counties, USA). In: Riegl BM, Dodge RE (eds) Coral reefs of the USA. Springer, Dordrecht, pp 175–220. doi:[10.1007/978-1-4020-6847-8_5](https://doi.org/10.1007/978-1-4020-6847-8_5)
- Beaman RJ, Daniell J, Harris PT (2005) Geology-benthos relationships on a temperate rocky bank, eastern Bass Strait, Australia. *Mar Freshwater Res* 56:943–958
- Bradley AP (1997) The use of the area under the ROC curve in the evaluation of machine learning algorithms. *Pattern Recogn* 30:1145–1159
- Brown CJ, Collier JS (2008) Mapping benthic habitat in regions of gradational substrata: an automated approach utilising geophysical, geological, and biological relationships. *Estuar Coast Shelf Sci* 78:203–214
- Brown CJ, Smith SJ, Lawton P, Anderson JT (2011) Benthic habitat mapping: a review of progress towards improved understanding of the spatial ecology of the seafloor using acoustic techniques. *Estuar Coast Shelf Sci* 92:502–520
- Buhl-Mortensen P, Buhl-Mortensen L (2004) Distribution of deep-water gorgonian corals in relation to benthic habitat features in the Northeast Channel (Atlantic Canada). *Mar Biol* 144:1223–1238
- Callaway R (2006) Tube worms promote community change. *Mar Ecol Prog Ser* 308:49–60
- Canepa G, Pace NG (2000) Seafloor segmentation from multibeam bathymetric sonar. In: Zakharia ME (ed) Proceedings of the fifth European conference on underwater acoustics, Lyon, France, pp 361–366
- Congalton RG (1991) A review of assessing the accuracy of classifications of remotely sensed data. *Remote Sens Environ* 37:35–46
- Daniell J, Siwabessy J, Nichol S, Brooke B (2015) Insight into environmental drivers of acoustic angular response using a self-organising map and hierarchical clustering. *Geo-Mar Lett* 35:387–403
- de Moustier CP, Alexandrou D (1991) Angular dependence of 12-kHz seafloor acoustic backscatter. *J Acoust Soc Am* 90(1):522–531
- de Moustier CP, Matsumoto H (1993) Seafloor acoustic remote sensing with multibeam echo-sounders and bathymetric sidescan sonar systems. *Mar Geophys Res* 15:27–42
- De Falco D, Tonielli R, Di Martino G, Innangi S, Simeone S, Parnum IM (2010) Relationships between multibeam backscatter, sediment grain size and *Posidonia oceanica* seagrass distribution. *Cont Shelf Res* 30:1941–1950
- Diesing M, Mitchell P, Stephens D (2016) Image-based seabed classification: what can we learn from terrestrial remote sensing? *ICES J Mar Sci* 73(10):2425–2441. doi:[10.1093/icesjms/fsw118](https://doi.org/10.1093/icesjms/fsw118)
- Dunlop J (1997) Statistical modelling of sidescan sonar images. In: Oceans 97. MTS/IEEE conference proceedings, vol 1, pp 33–38. doi:[10.1109/OCEANS.1997.634331](https://doi.org/10.1109/OCEANS.1997.634331)
- Erlandsson J, Kostylev V, Williams GA (1999) A field technique for estimating the influence of surface complexity on movement turtuosity in the tropical limpet *Cellana grata* gould. *Ophelia* 50:215–224
- Ferrini VL, Flood RD (2006) The effects of fine-scale surface roughness and grain size on 300 kHz multibeam backscatter intensity in sandy marine sedimentary environments. *Mar Geol* 228:153–172
- Fielding AH, Bell JF (1997) A review of methods for the assessment of prediction errors in conservation presence/absence models. *Environ Conserv* 24:38–49
- Fonseca L, Mayer L (2007) Remote estimation of surficial seafloor properties through the application angular range analysis to multibeam sonar data. *Mar Geophys Res* 28:119–126
- Fonseca L, Brown C, Calder B, Mayer L, Rzhavov Y (2009) Angular range analysis of acoustic themes from Stanton Banks Ireland: a link between visual interpretation and multibeam echosounder angular signatures. *Appl Acoust* 70(10):1289–1304
- Fortune J (2006) The grain size and heavy mineral content of sediment in Darwin Harbour. Aquatic Health Unit, Environmental Protection Agency, Darwin
- Gallaudet TC, de Moustier CP (2003) Highfrequency volume and boundary acoustic backscatter fluctuations in shallow water. *J Acoust Soc Am* 114(2):707–725
- Garza-Perez JR, Lehmann A, Arias-Gonzalez JE (2004) Spatial prediction of coral reef habitats: integrating ecology with spatial modeling and remote sensing. *Mar Ecol Prog Ser* 269:141–152
- Gavrilov AN, Parnum IM (2010) Fluctuations of seafloor backscatter data from multibeam sonar systems. *IEEE J Oceanic Eng* 35(2):209–219
- Gavrilov AN, Duncan AJ, McCauley RD, Parnum IM, Penrose JD, Siwabessy PJW, Woods AJ, Tseng Y-T (2005a) Characterization of the Seafloor in Australia's coastal zone using acoustic techniques. In: Proceedings of the international conference underwater acoustic measurements: technologies and results, Crete, Greece, pp 1075–1080
- Gavrilov AN, Siwabessy PJW, Parnum IM (2005b) Multibeam echosounder backscatter analysis. Centre for Marine Science and Technology, Perth
- Gensane M (1989) A statistical study of acoustic signals backscattered from the sea bottom. *IEEE J Oceanic Eng* 14(1):84–93
- Gray JS (1974) Animal-sediment relationships. *Oceanogr Mar Biol* 12:223–261
- Green MO, Hewitt JE, Thrush SF (1998) Seabed drag coefficient over natural beds of horse mussels (*Atrina zelandica*). *J Mar Res* 56:613–637
- Greene HG, Vallier TL, Bizzarro JJ, Watt S, Dieter BE (2007) Impacts of bay floor disturbances on benthic habitats in San Francisco Bay. In: Todd BJ, Greene HG (eds) Mapping the seafloor for habitat characterization, vol 47. Geological Association of Canada, St. Johns, pp 401–419
- Guevara-Fletcher CE, Cantera Kintz JR, Mejia-Ladina LM, Cortes FA (2011) Benthic macrofauna associated with submerged bottoms of a tectonic estuary in Tropical Eastern Pacific. *J Mar Biol*. doi:[10.1155/2011/193759](https://doi.org/10.1155/2011/193759)
- Guisan A, Zimmermann M (2000) Predictive habitat distribution models in ecology. *Ecol Model* 135:147–186
- Hamilton LJ, Parnum IM (2011) Acoustic seabed segmentation from direct statistical clustering of entire multibeam sonar backscatter curves. *Cont Shelf Res* 31:138–148
- Harris PT (2012) Surrogacy. In: Harris PT, Baker EK (eds) Seafloor geomorphology as benthic habitat. Elsevier, London, pp 93–108
- Harris PT, Baker EK (eds) (2012) Seafloor geomorphology as benthic habitat. Elsevier, London, pp 93–108
- Hasan RC, Ierodiaconou D, Laurenson L (2012) Combining angular response classification and backscatter imagery segmentation for benthic biological habitat mapping. *Estuar Coast Shelf Sci* 97:1–9
- Hellequin L, Boucher JM, Lurton X (2003) Processing of high-frequency multibeam echo sounder data for seafloor characterization. *IEEE J Oceanic Eng* 28(1):78–89
- Hillman JHT, Lamarche G, Pallentin A, Pecher IA, Gorman A, Schneider J (2017) Validation of automated supervised segmentation of multibeam backscatter data from the Chatham Rise, New Zealand. *Mar Geophys Res*. doi:[10.1007/s11001-016-9297-9](https://doi.org/10.1007/s11001-016-9297-9)
- Huang Z, Siwabessy J, Nichol SL, Anderson T, Brooke BP (2013) Predictive mapping of seabed cover types using angular

- response curves of multibeam backscatter data: testing different feature analysis approaches. *Cont Shelf Res* 61–62:12–22
- Huang Z, Siwabessy J, Nichol SL, Brooke BP (2014) Predictive mapping of seabed substrata using high-resolution multibeam sonar data: a case study from a shelf with complex geomorphology. *Mar Geol* 357:37–52
- Hughes-Clarke JE (1994) Toward remote seafloor classification using the angular response of acoustic backscattering: a case study from multiple overlapping GLORIA data. *IEEE J Oceanic Eng* 19(1):112–127
- Hughes-Clarke JE, Danforth BW, Valentine P (1997) Aerial seabed classification using backscatter angular response at 95 kHz. In: *Shallow Water, NATO SACLANTCEN, conference proceedings series CP, vol 45, pp 243–250*
- iXSurvey (2011) Bathymetric survey of Darwin Harbour. Hydrographic Survey Report D11-0219. iXSurvey Australia Pty Ltd, Brisbane
- Jackson DR, Winebrenner DP, Ishimaru A (1986) Application of the composite roughness model to high-frequency bottom backscatter. *J Acoust Soc Am* 79:1410–1422
- Jackson DR, Briggs KB, Williams KL, Richardson MD (1996) Tests of models for high-frequency seafloor backscatter. *IEEE J Oceanic Eng* 21(4):458–470
- Jakeman E, Tough RJA (1988) Non-Gaussian models for the statistics of the scattered waves. *Adv Phys* 37(5):471–529
- Ke X, Collins MB, Poulos SE (1994) Velocity structure and sea bed roughness associated with intertidal (sand and mud) flats and saltmarshes of the Wash, UK. *J Coastal Res* 10:702–715
- King IP (2016) RMA11—a three dimensional finite element model for water quality in estuaries and streams. Version 9.1a. Resource Modelling Associates, Sydney
- Kloser RJ, Keith G (2013) Seabed multi-beam backscatter mapping of the Australian continental margin. *Acoust Aust* 41(1):65–72
- Kloser RJ, Penrose JD, Butler AJ (2010) Multi-beam backscatter measurements used to infer seabed habitats. *Cont Shelf Res* 30:1772–1782
- Kostylev VE, Todd BJ, Fader GBJ, Courtney RC, Cameron GDM, Pickrill RA (2001) Benthic habitat mapping on the Scotian Shelf based on multibeam bathymetry, surficial geology and sea floor photographs. *Mar Ecol Prog Ser* 219:121–137
- Kostylev VE, Courtney RC, Robert G, Todd BJ (2003) Stock evaluation of giant scallop (*Placopecten magellanicus*) using high-resolution acoustics for seabed mapping. *Fish Res* 60(2–3):479–492
- Kracker L, Kendall M, McFall G (2008) Benthic features as a determinant for fish biomass in Gray's reef national marine sanctuary. *Mar Geodesy* 31:267–280
- Lamarche G, Lurton X, Verdier A-L, Augustin J-M (2010) Quantitative characterisation of seafloor substrate and bedforms using advanced processing of multibeam backscatter-application to Cook Strait, New Zealand. *Cont Shelf Res* 31(S-1):93–109
- Li J, Siwabessy J, Tran M, Huang Z, Heap A (2013) Predicting seabed hardness using random forest in R. In: Zhao Y, Cen Y (eds) *Data mining applications with R*. Elsevier, Amsterdam, pp 299–329
- Li J, Tran M, Siwabessy J (2016) Selecting optimal random forest predictive models: a case study on predicting the spatial distribution of seabed hardness. *PLoS ONE* 11(2):e0149089. doi:10.1371/journal.pone.0149089
- Lundblad ER, Wright DJ, Miller J, Larkin EM, Rinehart R, Naar DF, Donahue BT, Anderson SM, Battista T (2006) A benthic terrain classification scheme for American Samoa. *Mar Geodesy* 29:89–111
- Lurton X, Lamarche G (eds) (2015) Backscatter measurements by seafloor-mapping sonars. Guidelines and recommendations. Geohab Report. <http://geohab.org/publications/>
- Lyons AP, Abraham DA (1999) Statistical characterization of high-frequency shallow-water seafloor backscatter. *J Acoust Soc Am* 106(3):1307–1315
- Lyons AP, Anderson AL, Dwan FS (1994) Acoustic scattering from the seafloor: modeling and data comparison. *J Acoust Soc Am* 95(5):2441–2451
- McArthur MA, Brooke BP, Przeslawski R, Ryan DA, Lucieer VL, Nichol S, McCallum AW, Mellin C, Cresswell ID, Radke LC (2010) On the use of abiotic surrogates to describe marine benthic biodiversity. *Estuar Coast Shelf Sci* 88:21–32
- Mitchell NC (1993) A model for attenuation of backscatter due to sediment accumulations and its application to determine sediment thicknesses with GLORIA sidescan sonar. *J Geophys Res* 98:22477. doi:10.1029/93JB02217
- Nakamura Y, Sano M (2005) Comparison of invertebrate abundance in a seagrass bed and adjacent coral and sand areas at Amitori Bay, Iriomote Island, Japan. *Fish Sci* 71(3):543–550
- National Geophysical Data Center (2006) 2-Minute gridded global relief data (ETOPO2) v2. National Geophysical Data Center, NOAA. doi:10.7289/V5J1012Q
- Nichol SL, Anderson TJ, Battershill C, Brooke BP (2012) Submerged reefs and aeolian dunes as inherited habitats, Point Cloates, Carnarvon Shelf, Western Australia. In: Harris PT, Baker E (eds) *Atlas of seafloor geomorphology as habitat*. Elsevier, London
- Northern Territory Geological Survey (1988) Darwin 1:250,000 Geology Mapsheet SD5204, 2nd edn
- Novarini JC, Caruthers JW (1998) A simplified approach to backscattering from a rough seafloor with sediment inhomogeneities. *IEEE J Oceanic Eng* 23(3):157–166
- Parnum IM (2007) Benthic habitat mapping using multibeam sonar systems. Curtin University of Technology, Perth
- Parnum IM, Gavrilo AN (2011) High-frequency multibeam echosounder measurements of seafloor backscatter in shallow water: Part 1—Data acquisition and processing. *J Underw Technol* 30(1):3–12. doi:10.3723/ut.30.003
- Parnum IM, Siwabessy PJW, Gavrilo AN (2004) Identification of seafloor habitats in coastal shelf waters using a multibeam echosounder. In: *Acoustics 2004, proceedings of the conference of the Australian Acoustical Society, Gold Coast, Australia*, pp 181–186
- Parnum I, Gavrilo A, Siwabessy J, Duncan A (2006) Analysis of high-frequency multibeam backscatter statistics from difference seafloor habitats. In: *ECUA 8th European conference on underwater acoustics, Portugal*, pp 775–782
- Peterson G, Allen CR, Holling CS (1998) Ecological resilience, biodiversity and scale. *Ecosystems* 1:6–18
- Post AL, Wassenberg TJ, Passlow V (2006) Physical surrogates for macrofaunal distributions and abundance in a tropical gulf. *Mar Freshwater Res* 57:469–483
- Przeslawski R, Williams A, Nichol SL, Hughes MG, Anderson TJ, Althaus F (2011) Biogeography of the Lord Howe Rise region, Tasman Sea. *Deep-Sea Res II* 58(7–8):959–969. doi:10.1016/j.dsr2.2010.10.051
- Przeslawski R, Alvarez B, Kool J, Bridge T, Caley MJ, Nichol S (2015) Implications of sponge biodiversity patterns for the management of a marine reserve in northern Australia. *PLoS ONE* 10(11):e0141813. doi:10.1371/journal.pone.0141813
- Reise K (1981) Gnathostomulida abundant alongside polychaete burrows. *Mar Ecol Prog Ser* 6(3):329–333
- Siwabessy PJW, Parnum IM, Gavrilo A, McCauley RD (2006a) Overview of coastal water habitat mapping research for Coastal CRC. Coastal CRC Technical Report No. 86
- Siwabessy PJW, Gavrilo AN, Duncan AJ, Parnum IM (2006b) Statistical analysis of high-frequency multibeam backscatter data in shallow water. In: *Acoustics 2006, proceedings of the conference*

- of the Australasian Acoustical Societies, Christchurch, New Zealand, pp 507–514
- Siwabessy PJW, Daniell J, Li J, Huang Z, Heap AD, Nichol S, Anderson TJ, Tran M (2013) Methodologies for seabed substrate characterisation using multibeam bathymetry, backscatter and video data: a case study from the carbonate banks of the Timor Sea, Northern Australia. *Record* 2013/11. Geoscience Australia, Canberra
- Siwabessy PJW, Tran M, Huang Z, Nichol S, Atkinson I (2015) Mapping and classification of Darwin Harbour Seabed. *Record* 2015/18. Geoscience Australia, Canberra. doi:10.11636/Record.2015.018
- Smit N, Penny SS, Griffiths AD (2012) Assessment of marine biodiversity and habitat mapping in the Weddell region, Darwin Harbour. Report to the Department of Lands, Planning and Environment. Department of Land Resource Management, Palmerston
- Stanic S, Kennedy E (1992) Fluctuations of highfrequency shallow water seafloor reverberation. *J Acoust Soc Am* 91(4):1967–1973
- Stephens D, Diesing M (2014) A comparison of supervised classification methods for the prediction of substrate type using multibeam acoustic and legacy grain-size data. *PLoS ONE* 9:e93950
- Stewart WK, Chu D, Malik S (1994) Quantitative seafloor characterization using a bathymetric sidescan sonar. *IEEE J Oceanic Eng* 19(4):599–610
- Talukdar KK, Tyce RC, Clay CS (1995) Interpretation of Sea Beam backscatter data collected at the Laurentian fan off Nova Scotia using acoustic backscatter theory. *J Acoust Soc Am* 97(3):1545–1558
- Trevorrow MV (2004) Statistics of fluctuations in highfrequency low-grazing-angle backscatter from a rocky sea bed. *IEEE J Oceanic Eng* 29(2):236–245
- Tsuchiya M, Nishihira M (1986) Islands of *Mytilus edulis* as a habitat for small intertidal animals—effect of *Mytilus* age structure on the species composition of the associated fauna and community organization. *Mar Ecol Prog Ser* 31(2):171–178
- Van Rijn LC (2007) Unified view of sediment transport by currents and waves. I: initiation of motion, bed roughness, and bed-load transport. *J Hydraul Eng* 133(6):649–667
- Wedding LM, Friedlander AM, McGranaghan M, Yost RS, Monaco ME (2008) Using bathymetric lidar to define nearshore benthic habitat complexity: implications for management of reef fish assemblages in Hawaii. *Remote Sens Environ* 112:4159–4165
- Wentworth CK (1922) A scale of grade and class terms for clastic sediments. *J Geol* 30:377–392
- Williams KL, Jackson DR, Thorsos EI, Tang D, Briggs KB (2002) Acoustic backscattering experiments in a well characterized sand sediment: data/model comparisons using sediment fluid and Biot models. *IEEE J Oceanic Eng* 27(3):376–387
- Williams D, Wolanski E, Spagnol S (2006) Hydrodynamics of Darwin harbour. In: Wolanski E (ed) *Environments in Asia Pacific harbours*. Springer, Dordrecht, pp 461–476
- Wolstenholme J, Dinesen ZD, Alderslade P (1997) Hard corals of the Darwin Region, Northern Territory, Australia. In: Hanley JR, Caswell G, Megirian D, Larson HK (eds) *Proceedings of the sixth international marine biological workshop. The marine flora and fauna of Darwin Harbour, Northern Territory, Australia. Museums and Art Galleries of the Northern Territory and the Australian Marine Sciences Association, Darwin*, pp 391–398
- Woodroffe CD, Bardsley KN, Ward PJ, Hanley JR (1988) Production of mangrove litter in a macrotidal embayment, Darwin Harbour, NT, Australia. *Estuar Coast Shelf Sci* 26:581–598